Lepton correlations in gauge-boson pair production and decay

J. F. Gunion
Department of Physics, University of California, Davis, California 95616
and Institute for Theoretical Science, University of Oregon, Eugene, Oregon 97403

Z. Kunszt
Institute for Theoretical Physics, University of Bern, Sidlerstrasse 5, CH-3012 Bern, Switzerland
(Received 23 September 1985)

We present amplitude and cross-section formulas for fermion-antifermion annihilation to on-shell WW, WZ, ZZ, $W\gamma$, and $Z\gamma$ pairs in which the W and Z gauge bosons subsequently decay into fermion-antifermion pairs. The expressions include full spin-density-matrix correlations. This exact treatment yields fermion correlations that differ significantly from those obtained using W/Z-polarization-averaged cross sections followed by uncorrelated decay.

The polarization-averaged cross sections for production of WW, WZ, ZZ, $W\gamma$, and $Z\gamma$ pairs are well established.[1-6] A convenient summary appears in a paper by Eichten, Hinchliffe, Lane, and Quigg[7] (EHLQ). Gauge-boson production is an important test of the $SU(2)_L \times U(1)$ electroweak interaction theory as well as a source of background for new physics. Since W and Z inevitably decay to massless fermion-antifermion pairs it is apparent that correlations between the various fermions and antifermions in the final state will be of importance. In this article we present concise, fully covariant, and crossing-symmetric formulas for the processes

$$f_1\bar{f}_2 \to G \;(\to f_3\bar{f}_4) + G' \;(\to f_5\bar{f}_6)\,, \tag{1}$$

$$f_1\bar{f}_2 \to G \;(\to f_3\bar{f}_4) + \gamma\,, \tag{2}$$

which include full spin-density-matrix correlations. We shall take all fermions to be massless.

The calculations are most easily performed at the amplitude level for fixed external-particle helicities. We employ the techniques outlined in Ref. 8; they are closely related to those discussed in Refs. 9 and 10. We shall present results at the amplitude, and amplitude-squared levels. Because of cancellations required by gauge invariance, numerical programming is generally more conveniently done at the amplitude level.

The amplitudes will be presented in terms of the inner product defined and discussed in Ref. 8,

$$\langle p-|q+\rangle \equiv \langle pq\rangle = (p_-q_+)^{1/2}e^{i\phi_p} - (p_+q_-)^{1/2}e^{i\phi_q}\,,$$
$$\langle p-|q+\rangle^+ \equiv \langle pq\rangle^+ = \langle p^-|q^+\rangle^*\,, \tag{3}$$

for $p_0, q_0 > 0$. A crossing-invariant extension of these inner products to momenta of negative energy is defined by ($p_0, q_0 > 0$)

$$\langle(-p)q\rangle = i\langle pq\rangle\,,$$
$$\langle(-p)q\rangle^+ = i\langle pq\rangle^+\,, \tag{4}$$

see Ref. 8. Observe that $\langle p\,|\,q\rangle = -\langle q\,|\,p\rangle$. Remarkably all amplitudes for the processes of type (1) can be expressed in terms of a single function of these inner products. We define

$$F(1,2,3,4,5,6) = 4\langle 13\rangle\langle 26\rangle^+(\langle 15\rangle\langle 14\rangle^+ + \langle 35\rangle\langle 34\rangle^+)\,, \tag{5}$$

where we introduce the shorthand notation

$$\langle ij\rangle = \langle k_i k_j\rangle\,, \tag{6}$$

and k_i, $i = 1-6$, denote the four-momenta of the various fermions. Our particle labeling conventions for reactions (1) and (2) are given in Fig. 1. Note that all momenta and particles are taken to be outgoing in (5) and the other formulas to be presented: i.e.,

$$k_1 + k_2 + k_3 + k_4 + k_5 + k_6 = 0\,. \tag{7}$$

In addition particles 1, 3, and 5, must be fermions and particles 2, 4, and 6 antifermions when all are outgoing. Application to the specific processes of Fig. 1 requires crossing the 1 and 2 momenta that appear in our formulas to negative energy. For inner products the procedure is delineated in Eq. (4). [Suppose we consider the physical process

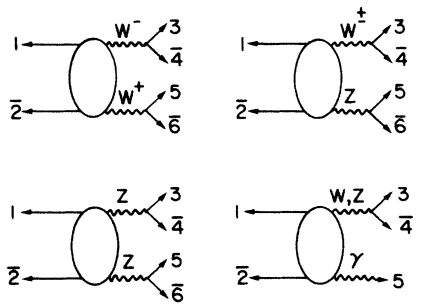

FIG. 1. Notation and conventions for the reactions of Eqs. (1) and (2).

$$\bar{u}(p_1)+u(p_2)\rightarrow \underset{\hookrightarrow e^-(p_3)\bar{\nu}_e(p_4)}{W^-} + \underset{\hookrightarrow \nu_\mu(p_5)\mu^+(p_6)}{W^+},$$

where all p's have positive energy. To apply our formulas define $k_1=-p_2$ and $k_2=-p_1$, $k_i=p_i$, $i=3$–6. In the outgoing sense particle 1 is $u(k_2)$ and particle 2 is $\bar{u}(k_1)$; quantum-number assignments in our formula are made accordingly. The inner product $\langle k_1 k_3\rangle$ would be evaluated as $\langle k_1 k_3\rangle=\langle(-p_2)p_3\rangle=i\langle p_2 p_3\rangle$.]

In presenting our formulas it is useful to define a variety of auxiliary quantities containing various coupling constants and propagators. These appear in Table I. The invariants appearing therein are defined by

$$s_{ij}=(k_i+k_j)^2,\quad s_{ijk}=(k_i+k_j+k_k)^2 . \tag{8}$$

In addition, the final-state W and Z propagators that are included in our amplitudes are evaluated on shell in the expressions of Table I. Finally our formulas do not include any color factors for initial- and final-state quarks; i.e., they apply to quarks of a given color.

For massless fermions helicity is conserved along a given fermion line in a Feynman diagram. All Feynman diagrams contributing to processes (1) and (2) are such that fermion 1 is connected to antifermion 2, 3 to 4, and 5 to 6. Thus, in the following, a helicity amplitude is completely specified by the value of the fermion helicities (λ_1, λ_3, and λ_5). The antifermion helicities (λ_2, λ_4, and λ_6, respectively) are determined by helicity conservation.

For WW production there are only two helicity amplitudes. In the notation of Fig. 1, λ_3 and λ_5 must be minus while λ_1 may be plus or minus. We obtain

$$A^{WW}(\lambda_1=-)=K_{WW}[\,a^{WW}F(1,2,3,4,5,6) - b^{WW}F(1,2,5,6,3,4)]\,, \tag{9a}$$

$$A^{WW}(\lambda_1=+)=K_{WW}c^{WW}[\,F(2,1,5,6,3,4) - F(2,1,3,4,5,6)]\,, \tag{9b}$$

where K_{WW}, a^{WW}, b^{WW}, and c^{WW} are defined in Table I; K_{WW} contains the on-shell pole factors for the two W's. The helicity amplitudes of (9) are easily squared and summed, yielding

$$\begin{aligned}|M|_{WW}^2=|A^{WW}(+)|^2+|A^{WW}(-)|^2=K_{WW}^2\{&I(1,2,3,4,5,6)\,|a^{WW}|^2+I(1,2,5,6,3,4)\,|b^{WW}|^2\\ &-J(1,2,3,4,5,6)\mathrm{Re}(a^{WW}b^{WW*})\\ &+[I(2,1,3,4,5,6)+I(2,1,5,6,3,4)-J(2,1,3,4,5,6)]\,|c^{WW}|^2\}\,.\end{aligned} \tag{10}$$

The normalization of $|M|^2$ is defined by the cross-section formula

$$d\sigma=\frac{1}{2s}\frac{1}{\text{color}}\frac{1}{\text{spin}}\sum_{\text{colors}}|M|^2 dR_4$$

with

$$dR_4=\prod_{i=3}^{6}\frac{d^3k_i}{(2\pi)^3 2k_i}(2\pi)^4\delta^4\left[k_1+k_2-\sum_{i=3}^{6}k_i\right].$$

TABLE I. Useful constants for cross-section formulas, Eqs. (9), (10), (14)–(17), and (21)–(24). U_{ij} = Cabibbo-Kobayashi-Maskawa-matrix entry as appropriate; $\tau_i=\pm1$ is twice the weak isospin; e_i = fractional charge; i labels the fermion. $M_{W,Z}$ and $\Gamma_{W,Z}$ are the masses and widths of the vector bosons. The variables s_{ij} and s_{ijk} are defined in Eq. (8). The fine-structure constant of QED is α, and θ_W is the Weinberg angle.

$x_W=\sin^2\theta_W$ $L_i=\tau_i-2e_i x_W$	$R_i=-2e_i x_W$ $e^2=4\pi\alpha$
$d^{WW}=L_1\dfrac{M_Z^2}{s_{12}(s_{12}-M_Z^2)}+\dfrac{\tau_1}{s_{12}}$	$c^{WW}=R_1\dfrac{M_Z^2}{s_{12}(s_{12}-M_Z^2)}$
$a^{WW}=d^{WW}+\dfrac{(\tau_1+1)}{2s_{134}}$	$b^{WW}=d^{WW}+\dfrac{(\tau_1-1)}{2s_{156}}$
$K_{WW}=U_{34}U_{56}\dfrac{e^4}{4x_W^2}\dfrac{1}{M_W^2\Gamma_W^2}$	$K_{WZ}=\dfrac{U_{12}U_{34}e^4}{8x_W^2(1-x_W)}\dfrac{1}{M_W\Gamma_W M_Z\Gamma_Z}$
$a^{WZ}=\dfrac{L_2}{s_{134}}-\dfrac{\tau_1 2(1-x_W)}{s_{12}-M_W^2}$	$b^{WZ}=\dfrac{L_1}{s_{156}}+\dfrac{\tau_1 2(1-x_W)}{s_{12}-M_W^2}$
$K_{ZZ}=\dfrac{e^4}{16x_W^2(1-x_W)^2}\dfrac{1}{M_Z^2\Gamma_Z^2}$	$K_{W\gamma}=\dfrac{U_{12}U_{34}e^3}{2x_W M_W\Gamma_W}$
$K_{Z\gamma}=\dfrac{e^3}{4x_W(1-x_W)}\dfrac{1}{M_Z\Gamma_Z}$	

TABLE II. The functions I and J of Eq. (11) in terms of dot products.

$$I(1,2,3,4,5,6)=256(k_1\cdot k_3)(k_2\cdot k_6)[(k_4\cdot k_{13})(k_5\cdot k_{13})-(k_4\cdot k_5)(k_1\cdot k_3)]$$
$$J(1,2,3,4,5,6)=-64(k_{135})^2[(k_5\cdot k_6)V_{1243}-(k_5\cdot k_2)V_{1643}+(k_5\cdot k_4)V_{1623}-(k_5\cdot k_3)V_{1624}+(k_5\cdot k_1)V_{3624}]$$
$$-512(k_1\cdot k_3)(k_1\cdot k_5)(k_2\cdot k_4)(k_2\cdot k_6)$$
$$k_{ijl}=k_i+k_j+k_l \quad k_{ij}=k_i+k_j$$
$$V_{ijlm}=(k_i\cdot k_j)(k_l\cdot k_m)-(k_i\cdot k_l)(k_j\cdot k_m)+(k_i\cdot k_m)(k_j\cdot k_l)$$

The quantities I and J are given by

$$I(1,2,3,4,5,6)=|F(1,2,3,4,5,6)|^2 \tag{11a}$$

and

$$J(1,2,3,4,5,6)=2F(1,2,3,4,5,6)F^*(1,2,5,6,3,4)\ . \tag{11b}$$

The functions $I(1,2,3,4,5,6)$ and $J(1,2,3,4,5,6)$ appear in Table II. From the simple structure of Eq. (9) we can easily see the rather intriguing cancellation mechanism at high energy ($E\gg 2M_W$) required by gauge invariance. We find complete cancellation between the γ and Z contributions in the coefficient c^{WW} while they cancel only partially in the coefficients a^{WW} and b^{WW}. In the helicity amplitude $A^{WW}(-)$ the cancellation becomes complete, due to a further cancellation between the two terms of Eq. (9a). This can be easily seen assuming some particular collinear configuration for k_3,k_4, and k_5,k_6 (allowed in the high-energy limit).

We emphasize that the second cancellation is not made manifest analytically in Eqs. (9a), (9b), and (10); this could potentially lead to numerical difficulties. However, the problem is not significant at the amplitude level of Eq. (9). [In practice Eq. (9) and, for many purposes, Eq. (10) can be used up to Superconducting Super Collider energies. The number of decimal digits lost to inaccuracy in the cancellation computation for Eq. (9) is $\sim\ln(\hat{s}/4M_W{}^2)$, while it is $\sim\ln(\hat{s}/4M_W{}^2)^2$ for Eq. (10); $\hat{s}$ is the subprocess center-of-mass energy squared. If necessary the cancellations in Eq. (10) can be made analytically by algebraically converting to a minimal set of independent invariants over a common denominator.]

It is an interesting exercise to reproduce the standard polarization summed formula for WW pair production; for a convenient form see (4.48) of EHLQ. We integrate Eq. (10) over the fermion-antifermion angular variables for the two W decays (as defined in the respective W rest frames). We define

$$X_I(t,u,m_{34}{}^2,m_{56}{}^2)=\frac{1}{\kappa}\int d\phi_{34}d\phi_{56}I(1,2,3,4,5,6)\ ,$$
$$X_J(t,u,m_{34}{}^2,m_{56}{}^2)=\frac{1}{\kappa}\int d\phi_{34}d\phi_{56}J(1,2,3,4,5,6)\ , \tag{12}$$

where

$$d\phi_{ij}(k_{ij})=\frac{d^3k_i}{2k_i}\frac{d^3k_j}{2k_j}\delta^4(k_{ij}-k_i-k_j)\ ,$$
$$\kappa=\tfrac{4}{9}(\pi/2)^2,\quad t=(k_1+k_{34})^2,\quad u=(k_1+k_{56})^2\ , \tag{13}$$

and we have defined $k_{ij}=k_i+k_j$. The functions X_I and X_J appear in Table III. The cross section $d\sigma/dt(1+2\to W+W)$ is directly obtained from Eq. (10) (up to various spin, color, and other normalization factors) by replacing I and J by X_I and X_J, including the product $(\pi m_{34}\Gamma_{34})(\pi m_{56}\Gamma_{56})$ $(=\pi^2M_W{}^2\Gamma_W{}^2$ in the present case), and summing over a complete set of decay channels. These last two steps serve to cancel the on-pole $(M_W{}^2\Gamma_W{}^2)^{-2}$ factor present in $|K_{WW}|^2$.

Turning to WZ production there are, again, only two helicity amplitudes. For all diagrams it is necessary that $\lambda_3=-$ and $\lambda_1=-$, whereas λ_5 may be $+$ or $-$ (see Fig. 1 for notation). As before, the antifermion helicities λ_2, λ_4, and λ_6 are determined through helicity conservation by λ_1, λ_3, and λ_5, respectively. We obtain

$$A^{WZ}(\lambda_5=-)=K_{WZ}L_5[a^{WZ}F(1,2,3,4,5,6)+b^{WZ}F(1,2,5,6,3,4)]\ ,$$
$$A^{WZ}(\lambda_5=+)=K_{WZ}R_5[a^{WZ}F(1,2,3,4,6,5)+b^{WZ}F(1,2,6,5,3,4)]\ , \tag{14}$$

where K_{WZ}, L, R, a^{WZ}, and b^{WZ} appear in Table I. The amplitude squared is computed as

$$|M|_{WZ}{}^2=|A^{WZ}(-)|^2+|A^{WZ}(+)|^2 \tag{15}$$

and may be written in terms of the I and J functions defined in Eq. (11). As discussed for WW production the two terms in the formulas of Eq. (14) tend to cancel at high subprocess energy, $(\hat{s})^{1/2}$. Thus far greater numerical accuracy is obtained by first computing the amplitudes numerically using Eq. (14) and then squaring and summing as in Eq. (15). Finally, we note that by using (11), (12), (14), and (15), according to the procedure outlined

TABLE III. The functions X_I and X_J of Eq. (12).

$$t=s_{134}\quad u=s_{156}$$

$$H(t,u,m_{34}{}^2,m_{56}{}^2)\equiv\frac{tu}{m_{34}{}^2m_{56}{}^2}-2\left[\frac{1}{m_{34}{}^2}+\frac{1}{m_{56}{}^2}\right](t+u)+2\left[\frac{m_{34}{}^2}{m_{56}{}^2}+\frac{m_{56}{}^2}{m_{34}{}^2}\right]$$

$$X_I(t,u,m_{34}{}^2,m_{56}{}^2)=-4m_{34}{}^2m_{56}{}^2+t(3t+u)+t^2H(t,u,m_{34}{}^2,m_{56}{}^2)$$

$$X_J(t,u,m_{34}{}^2,m_{56}{}^2)=8(m_{34}{}^2+m_{56}{}^2)^2-8(m_{34}{}^2+m_{56}{}^2)(t+u)-6tu-2tuH(t,u,m_{34}{}^2,m_{56}{}^2)$$

for the WW case, we algebraically reproduce the unpolarized WZ cross section, Eq. (4.60) of EHLQ.

For ZZ pair production, all possible helicity choices for λ_1, λ_3, and λ_5 are allowed, a total of eight helicity amplitudes. Each receives contributions from two diagrams. We give below the results for the amplitudes $A^{ZZ}(\lambda_1,\lambda_3,\lambda_5)$;

$$A^{ZZ}(-,-,-)=L_3L_5L_1{}^2K_{ZZ}\left[\frac{F(1,2,3,4,5,6)}{s_{134}}+\frac{F(1,2,5,6,3,4)}{s_{156}}\right],$$

$$A^{ZZ}(-,+,-)=R_3L_5L_1{}^2K_{ZZ}\left[\frac{F(1,2,4,3,5,6)}{s_{134}}+\frac{F(1,2,5,6,4,3)}{s_{156}}\right],$$

$$A^{ZZ}(-,-,+)=L_3R_5L_1{}^2K_{ZZ}\left[\frac{F(1,2,3,4,6,5)}{s_{134}}+\frac{F(1,2,6,5,3,4)}{s_{156}}\right],$$

$$A^{ZZ}(-,+,+)=R_3R_5L_1{}^2K_{ZZ}\left[\frac{F(1,2,4,3,6,5)}{s_{134}}+\frac{F(1,2,6,5,4,3)}{s_{156}}\right]. \tag{16}$$

The remaining four helicity amplitudes are obtained by the replacement

$$A^{ZZ}(+,\lambda_3,\lambda_5)=A^{ZZ}(-,\lambda_3,\lambda_5;L_1\to R_1,1\leftrightarrow 2 \text{ in } F\text{'s}) . \tag{17}$$

We obtain the full amplitude squared as

$$|M|_{ZZ}{}^2=\sum_{\lambda_1=\pm,\lambda_3=\pm,\lambda_5=\pm}|A^{ZZ}(\lambda_1,\lambda_3,\lambda_5)|^2 . \tag{18}$$

A discussion analogous to the WW and WZ cases, regarding cancellations and the two means for implementing $|M|_{ZZ}{}^2$ computations, applies in this case as well. Also, by using Eqs. (11), (12), and (16)–(18), according to the procedure outlined for the WW and WZ cases, we algebraically reproduce the unpolarized ZZ cross section, Eq. (4.69) of EHLQ.

For completeness we also give the amplitudes and cross sections for the reactions (2). The notation and particle labeling is defined in Fig. 1. The reactions (2) can again all be expressed in terms of a single function,

$$C(1,2,3,4,5)=\frac{2\sqrt{2}\langle 13\rangle^2\langle 34\rangle^+}{\langle 15\rangle\langle 25\rangle} , \tag{19}$$

via argument permutation. However, every amplitude turns out to have the common dynamical factor

$$\delta=\frac{2(2)^{1/2}\langle 34\rangle^+}{\langle 15\rangle\langle 25\rangle} , \tag{20}$$

where, up to a phase, $\langle 34\rangle^+=M_W$ or M_Z for $W\gamma$ or $Z\gamma$, respectively. In terms of δ we obtain the simplest amplitude expressions.

For the $W\gamma$ case $\lambda_1=\lambda_3=-$ is required while $\lambda_\gamma=\pm$ is allowed. We obtain

$$A^{W\gamma}(\lambda_\gamma=+)=K_{W\gamma}\{e_2-\tau_1[s_{25}/(s_{12}-M_W{}^2)]\}\delta\langle 13\rangle^2 ,$$
$$A^{W\gamma}(\lambda_\gamma=-)=K_{W\gamma}\{e_2-\tau_1[s_{25}/(s_{12}-M_W{}^2)]\}\delta\langle 24\rangle^2 . \tag{21}$$

Squaring and summing the amplitudes of (19) leads to

$$|M|_{W\gamma}{}^2=8|K_{W\gamma}|^2M_W{}^2\frac{s_{13}{}^2+s_{24}{}^2}{s_{15}s_{25}}\times\left[e_2-\tau_1\frac{s_{25}}{s_{12}-M_W{}^2}\right]^2 . \tag{22}$$

Note the presence of the well-known radiation zero in (21) and (22).[11] The result (22) is in agreement with the formula of Ref. 12. Once again we easily reproduce the polarization-averaged formula, Eq. (4.77) of EHLQ, by integrating over the fermion-antifermion decay angle in the W center of mass, correcting for the on-shell propagator factor in $K_{W\gamma}$, performing appropriate color sums, and color-spin averaging.

For $Z\gamma$ we have allowed helicities $\lambda_1=\pm$, $\lambda_3=\pm$, $\lambda_\gamma=\pm$. We give the amplitudes $A^{Z\gamma}(\lambda_1,\lambda_3,\lambda_\gamma)$ below;

$$A^{Z\gamma}(-,-,+)=K^{Z\gamma}\delta e_1L_1L_3\langle 13\rangle^2 ,$$
$$A^{Z\gamma}(-,+,+)=K^{Z\gamma}\delta e_1L_1R_3\langle 14\rangle^2 ,$$
$$A^{Z\gamma}(+,-,+)=K^{Z\gamma}\delta e_1R_1L_3\langle 23\rangle^2 ,$$
$$A^{Z\gamma}(+,+,+)=K^{Z\gamma}\delta e_1R_1R_3\langle 24\rangle^2 . \tag{23}$$

The amplitudes for $\lambda_\gamma=-$ can be obtained from (23) by the relation

$$A^{Z\gamma}(\lambda_1,\lambda_3,-;1,2,3,4,5)=e^{i\eta}A^{Z\gamma}(\lambda_1,\lambda_3,+;2,1,4,3,5) , \tag{24}$$

where $e^{i\eta}$ is an unimportant phase factor, and δ is unchanged by the symmetry operation. Squaring and summing the eight helicity amplitudes yields

$$|M|_{Z\gamma}{}^2=K_{Z\gamma}{}^2\frac{8M_Z{}^2}{s_{12}s_{25}}e_1{}^2[(L_1{}^2L_3{}^2+R_1{}^2R_3{}^2)(s_{13}{}^2+s_{24}{}^2)+(L_1{}^2R_3{}^2+L_3{}^2R_1{}^2)\times(s_{14}{}^2+s_{23}{}^2)] . \tag{25}$$

Again the EHLQ formula, Eq. (4.79), can be obtained following the decay integration procedure outlined for the $W\gamma$ case.

We wish to emphasize once again that the $|M|^2$ forms presented for the five reactions of (1) and (2) are for fermions of a given flavor and color (if appropriate) including couplings for the W and Z decay and including the W/Z pole(s) evaluated on shell. The branching ratios for

the fermion decays of the gauge bosons are, thus, automatically present.

Finally we illustrate the importance of including the final-state fermion correlations by several examples. As a first extreme example consider WW production according to Eq. (9). Assume that the fermion -1 is polarized with $\lambda_1=+$. In the center of mass of the WW system if the W's decay in such a way that fermion -3 of the W^- decay moves parallel to p_{W^-} and fermion -5 of the W^+ decay moves antiparallel to p_{W^+}, then the full four-momenta of fermions 3 and 5 and of antifermions 4 and 6 are, respectively, proportional. In this case

$$F(1,2,3,4,5,6)=F(1,2,5,6,3,4)$$

and the amplitude of Eq. (9b) and corresponding cross section vanish. This result is obviously not obtained by taking the WW-polarization-averaged cross section (for fixed initial fermion helicity) followed by uncorrelated W decays.

As further examples, we present three figures which illustrate the correlation between the charged lepton and antilepton emerging from the reactions

$$e^-e^+ \to W^- \;(\to l\bar{\nu}_l) + W^+ \;(\to \bar{l}'\nu_{l'}) \tag{26}$$

and

$$\bar{p}p \text{ or } pp \to W^- \;(\to l\bar{\nu}_l) + W^+ \;(\to \bar{l}'\nu_{l'}) \,. \tag{27}$$

In the latter cases full distribution function folding using EHLQ $N_{\text{set}}=2$ has been performed. Appropriate spin averages for (25) and (26), and color sum and averages for (26) are included. We first define three variables of interest:

$$M_{l,\bar{l}'}=(p_l+p_{\bar{l}'})^2 \,, \tag{28a}$$

$$\phi=\arccos(\hat{\mathbf{p}}_l^{\,T}\cdot\hat{\mathbf{p}}_{\bar{l}'}^{\,T}) \,, \tag{28b}$$

$$\Delta y=y_l-y_{\bar{l}'} \,. \tag{28c}$$

The first is the effective mass of the $l/\bar{l}'$ pair, the second is the relative angle between l and $\bar{l}'$ in the transverse plane, and the third is the difference of the l and $\bar{l}'$ rapidities. In all the figures we compare the distributions, in one or more of these variables, as derived from our exact formula, Eq. (10), to those obtained using the polarization summed EHLQ formula followed by uncorrelated W decays. Minimal cuts on the l and $\bar{l}'$ transverse momenta and rapidities are made as indicated on the figures. Cross sections correspond to a single $l/\bar{l}'$ decay channel for the W^-/W^+. Integrated cross sections (subject to the indicated cuts) appear in the figure captions.

In Fig. 2 we plot the $M_{l,\bar{l}'}$ and ϕ distributions for reaction (25) at $\sqrt{s}=200$ GeV. Substantial differences between the exact and uncorrelated decay results are apparent. For instance, the exact ϕ distribution is much steeper than that predicted in the approximate treatment. The integrated cross section of roughly 0.1 pb combined with a luminosity of $10^{32}/\text{cm}^2\,\text{sec}$ at a facility of the type of CERN LEP II implies that such distributions would be fully amenable to measurement.

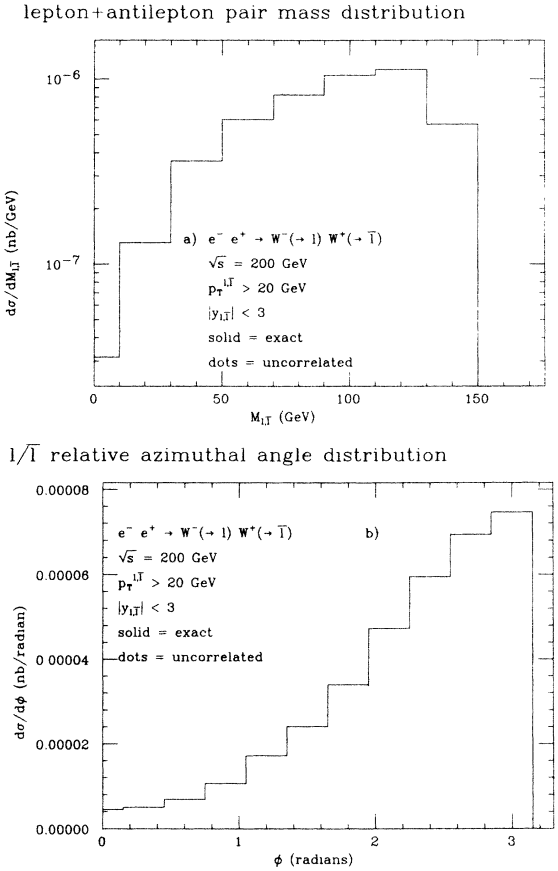

FIG. 2. Comparison of exact and uncorrelated decay distributions in $M_{l,\bar{l}'}$ and ϕ for e^-e^+ collisions at $\sqrt{s}=200$ GeV. The integrated cross sections, subject to the cuts indicated, are $\sigma_{\text{exact}}=0.094$ pb, $\sigma_{\text{uncorrelated}}=0.086$ pb. Uncut cross sections are 10% higher.

In Fig. 3 we plot ϕ and Δy distributions for pp collisions, Eq. (26), at $\sqrt{s}=2$ TeV. Substantial differences between exact and uncorrelated decay results appear. (In contrast the difference in $M_{l,\bar{l}'}$ spectra is, now, minimal.) However, the integrated cross section, subject to our cuts, is only 0.03 pb. (Removing the cuts leads to only a 10–20% increase.) This implies that the expected Fermilab Tevatron luminosity of $1-10$ pb^{-1}/yr will not allow measurements of these spectra in the purely leptonic modes. Even including quark decay channels for the W's (and the color sum factor of 3 for each quark flavor) leads to rather few events. In addition, such hadronic modes will have substantial QCD backgrounds.[13,14]

Finally in Fig. 4 we present ϕ and Δy distributions for pp collisions at $\sqrt{s}=40$ TeV. [Note that at a luminosity of $L\geq 10^{32}/\text{cm}^2\,\text{sec}$ the integrated cross section of roughly 0.13 pb (with the indicated cuts) at $\sqrt{s}=40$ TeV implies that such distributions can be measured.] Only the ϕ distribution shows a significant difference between the exact and uncorrelated decay calculations. In general the difference between the two treatments decreases as the range of subprocess energies being integrated over increases. This trend is made particularly obvious by comparing the three ϕ distributions; the greater steepness of the exact calcula-

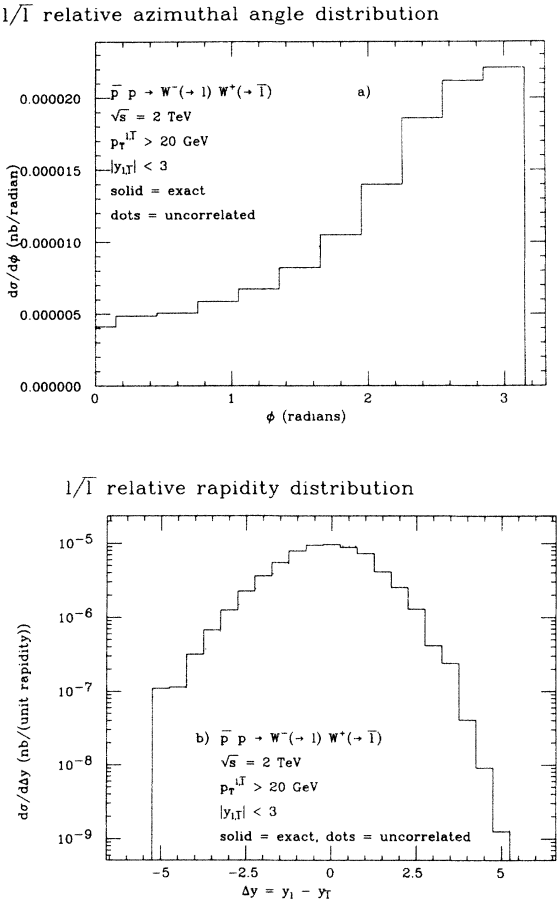

FIG. 3. Comparison of exact and uncorrelated decay distributions in ϕ and Δy for $\bar{p}p$ collisions at $\sqrt{s}=2$ TeV. Integrated cross sections including cuts are $\sigma_{\text{exact}}=0.033$ pb, $\sigma_{\text{uncorrelated}}=0.034$ pb. Uncut cross sections are 10% higher.

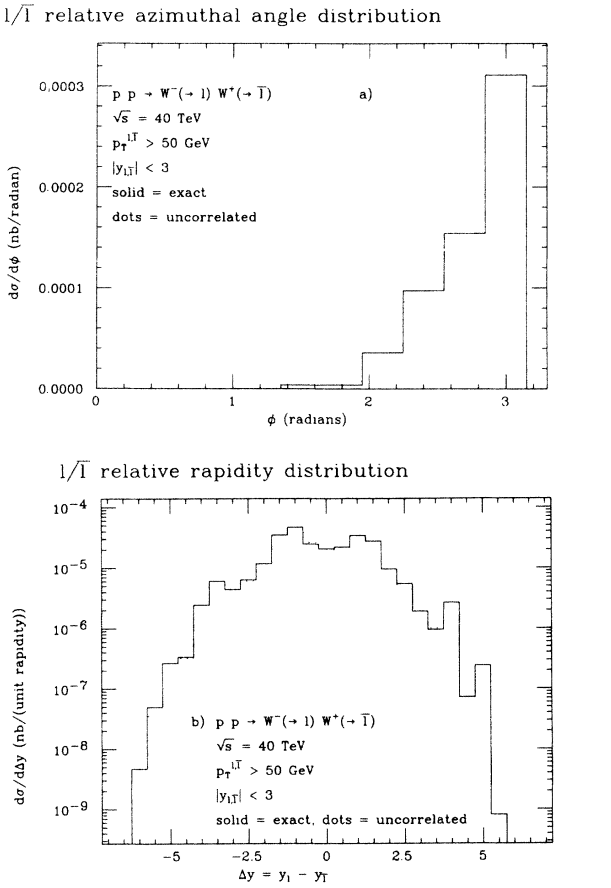

FIG. 4. Comparison of exact and uncorrelated decay distributions in ϕ and Δy for pp collisions at $\sqrt{s}=40$ TeV. Integrated cross sections including cuts are $\sigma_{\text{exact}}=0.13$ pb, $\sigma_{\text{uncorrelated}}=0.11$ pb. Uncut cross sections are a factor of 10 larger and exhibit less difference between the two treatments.

tion distribution slowly diminishes in going from Fig. 2 to Fig. 4.

We note that, in the above numerical calculations, we did not experience any difficulty due to cancellations in using the amplitude-squared formula, Eq. (10). This is because the average subprocess energy is modest compared to $2M_W$ in all cases. Applications involving large subprocess energy could require programming at the amplitude level of Eq. (9).

In conclusion, it is clear that an exact treatment of spin correlations, as incorporated in our formulas, is in most cases necessary for predicting many of the features of gauge-boson pair production and decay.

We would like to thank the Oregon Workshop on Super High Energy Physics for supporting this work. One of us (Z.K.) thanks the Central Research Institute of Physics, Budapest, for an extended leave of absence. This work was supported by the Department of Energy and Z.K. was supported by Sweizerische Nationfonds.

[1]W. Alles, Ch. Boyer, and A. J. Buras, Nucl. Phys. **B119**, 125 (1977).
[2]R. W. Brown and K. O. Mikaelian, Phys. Rev. D **19**, 922 (1979).
[3]R. W. Brown, D. Sahdev, and K. J. O. Mikaelian, Phys. Rev. D **20**, 1164 (1979).
[4]K. F. J. Gaemers and G. J. Gounaris, Z. Phys. C **1**, 259 (1979).
[5]F. Renard, Nucl. Phys. **B196**, 93 (1982).
[6]K. O. Mikaelian, M. A. Samuel, and D. Sahdev, Phys. Rev. Lett. **43**, 746 (1979).
[7]E. Eichten, I. Hinchliffe, K. Lane, and C. Quigg, Rev. Mod. Phys. **56**, 579 (1984).
[8]J. F. Gunion and Z. Kunszt, Phys. Lett. **161B**, 333 (1985).
[9]CALCUL collaboration, P. De Causmaecker, R. Gastmans, W. Troust, and T. T. Wu, Phys. Lett. **105B**, 215 (1981); Nucl. Phys. **B206**, 53 (1982); F. A. Berends *et al.*, *ibid.* **B206**, 61 (1982); **B239**, 382 (1984).
[10]R. Kleiss and W. J. Stirling, Report No. CERN-TH 4184/85, 1985 (unpublished).
[11]K. Hagiwara, F. Halzen, and F. Herzog, Phys. Lett. **135B**,

324 (1984); S. J. Brodsky and R. W. Brown, *ibid.* **49**, 966 (1982); R. W. Brown, K. L. Kowalski, and S. J. Brodsky, Phys. Rev. D **28**, 624 (1983).

[12]J. Cortes, K. Hagiwara, and F. Herzog, Phys. Rev. D **28**, 2311 (1984).

[13]W. J. Stirling, R. K. Kleiss, and S. D. Ellis, Report CERN-TH 4209/85, 1985 (unpublished).

[14]J. F. Gunion, Z. Kunszt, and M. Soldate, Phys. Lett. B (to be published).